Chinese Journal of Aeronautics, 2013,26(4): 986–992

Chinese Society of Aeronautics and Astronautics
& Beihang University

Chinese Journal of Aeronautics

cja@buaa.edu.cn
www.sciencedirect.com

An approach for parameter estimation of combined CPPM and LFM radar signal

Zhang Wei, Xiong Ying, Wang Pei, Wang Jun, Tang Bin *

School of Electronic and Information Engineering, University of Electronic Science and Technology of China, Chengdu 611731, China

Received 20 April 2012; revised 9 July 2012; accepted 28 November 2012
Available online 3 July 2013

KEYWORDS

Chaotic pulse position modulation;
Combined radar signal;
Cyclic autocorrelation;
Electronic countermeasures;
Hough transform;
Linear frequency modulation;
Volterra adaptive filter

Abstract In this paper, the problem of parameter estimation of the combined radar signal adopting chaotic pulse position modulation (CPPM) and linear frequency modulation (LFM), which can be widely used in electronic countermeasures, is addressed. An approach is proposed to estimate the initial frequency and chirp rate of the combined signal by exploiting the second-order cyclostationarity of the intra-pulse signal. In addition, under the condition of the equal pulse width, the pulse repetition interval (PRI) of the combined signal is predicted using the low-order Volterra adaptive filter. Simulations demonstrate that the proposed cyclic autocorrelation Hough transform (CHT) algorithm is theoretically tolerant to additive white Gaussian noise. When the value of signal noise to ratio (SNR) is less than −4 dB, it can still estimate the intra-pulse parameters well. When SNR = −3 dB, a good prediction of the PRI sequence can be achieved by the Volterra adaptive filter algorithm, even only 100 training samples.

1. Introduction

The combined chaotic pulse position modulation linear frequency modulation (CPPM-LFM) signal has attracted significant attention recently. It has been widely applied to stealth radar, sonar and communication systems because of its good performance of target detection, low probability of intercept (LPI)[1] and superior resolution. It is followed that this signal has two characteristics. On the one hand, the carrier frequency of the intra-pulse varies linearly. On the other hand, the pulse position is modulated by chaotic sequence. Due to the aperiodic interval, this signal is difficult to be observed by the reconnaissance system. The literatures for the contemporary study focus on the LFM signal and CPPM signal. So far, there are few detection and estimation schemes for this combined signal.

In this paper, the CPPM-LFM signal is analyzed with respect to its structural property. It is easily found that the intra pulse parameters can be estimated through the conventional estimation algorithms[2–4] in the presence of one intercepted pulse. However, the estimates are relatively dispersed with a large variance via the cycle placidity method[3] when signal to noise (SNR) is low. In view of the fact that the key attractive attributes of Hough transform (HT) are the capability of extracting signal feature as well as the good performance of anti-noise interference, we proposed a parameter estimation approach for CPPM-LFM intra pulse signal on the basis of cyclic autocorrelation-Hough transform (CHT).

* Corresponding author. Tel.: +86 28 61830432.
E-mail address: bint@uestc.edu.cn (B. Tang).

Peer review under responsibility of Editorial Committee of CJA.

ELSEVIER Production and hosting by Elsevier

1000-9361 © 2013 Production and hosting by Elsevier Ltd. on behalf of CSAA & BUAA. Open access under CC BY-NC-ND license.
http://dx.doi.org/10.1016/j.cja.2013.06.008

In addition, under the conditions of equal pulse width, the main idea underlying CPPM is to modulate a pulse train by alteration of pulse repetition interval (PRI) with respect to a chaotic discrete sequence. It leads to the result that the combined signal is easily mistaken as LFM signals of multiple radars by the reconnaissance receiver. The conventional recognition and sorting algorithms are no more applicable. Therefore, the pulse position prediction of this signal is still an open problem. However, in the existent literature, scholars pay significant attention to the analysis of the superior properties of CPPM signal and the basic design principles for chaotic-pulse generator.[1,5,6] In this paper, according to the nonlinear generation mechanism and short-term predictability of the chaotic signal, it can be modeled as nonlinear architecture to predict the following pulse position. There are mainly two nonlinear schemes: neural networks and Volterra series expansion. Compared with the neural networks in computational burden, the Volterra filter has the advantage and can deal with a class of nonlinear systems[7]. From a practical viewpoint of radar reconnaissance receiver, the second-order zVolterra (SOV)[8,9] and the third-order Volterra (TOV)[10,11] prediction filters are analyzed and established as prediction architectures for PRI. Note that the output of Volterra system is linearly dependent upon its kernel coefficients, least mean square (LMS)-based kernel identification algorithm is suggested. The feasibility and effectiveness of the algorithms are demonstrated by theoretical analysis and simulation results.

2. Signal model

In fact, the CPPM-LFM radar signal can be modeled as

$$s(t)=\frac{1}{\sqrt{L}}\sum_{l=0}^{L-1}u(t-c_l+\varepsilon_l)x(t) \tag{1}$$

where $u(t)=\begin{cases}1/\sqrt{T_L}, & 0\leqslant t<T_L\\ 0, & \text{otherwise}\end{cases}$ is the subpulse with the pulse width T_L, L the pulse number. $x(t)=A\mathrm{e}^{\mathrm{j}[2\pi(f_0t+\frac{1}{2}Kt^2)+\varphi_0]}$, A is the signal amplitude, f_0 the initial frequency, K the chirp rate, φ_0 the initial phase. c_l, chaotic sequence, is the position of the lth pulse, under the conditions of the equal pulse width, PRI, i.e., $(c_{l+1}-c_l)$ is also the chaotic sequence. ε_l is the error sequence of pulse position modulation, without loss of generality, we assume $\varepsilon_l=0$.

For ease of analysis and comment, the combined signal $s(t)$ can be decomposed as intra and inter pulse parts. Aimed at the cyclic property of the signal, the intra pulse in one cycle can be expressed as

$$x_{\mathrm{s}}(t)=x(t)+n(t) \tag{2}$$

where $n(t)$ is a zero-mean white Gaussian noise that is independent of $x(t)$. Therefore, the parameter estimation algorithm will be concentrated on a LFM signal, and high precision in low SNR is of interest.

The inter-pulse part consists of the PRI sequence. Pulse position prediction derived from the PRI prediction is detailed in Section 4, which is essential to further signal sorting and tracking.

3. Initial frequency and chirp rate estimation based on the CHT method

3.1. Cyclic autocorrelation algorithm

From Eq. (2), the single pulse signal is a LFM signal, which has been proven to be cyclostationary, and its time-varying autocorrelation function is given by

$$\begin{aligned}R_{\mathrm{s}}(t-\tau/2,t+\tau/2)&=E\{x_{\mathrm{s}}(t-\tau/2)x_{\mathrm{s}}^{*}(t+\tau/2)\}\\&=A^2\mathrm{e}^{-\mathrm{j}2\pi(f_0\tau+K t\tau)}+R'_{\mathrm{n}}(\tau)\end{aligned} \tag{3}$$

where $E\{\bullet\}$ is the expectation operator, and $R'_{\mathrm{n}}(\tau)$ the noise after the autocorrelation process. When the number of sample points is large enough, it can be considered as complex Gaussian noise according to the central limit theorem.

Since $R_{\mathrm{s}}(t-\tau/2,\ t+\tau/2)$ is periodic, it admits a Fourier series representation,

$$\begin{aligned}R_{\mathrm{s}}^{\alpha}(\tau)&=\lim_{T\to\infty}\frac{1}{T}\int_{-T/2}^{+T/2}R_{\mathrm{s}}(t-\tau/2,t+\tau/2)\mathrm{e}^{-\mathrm{j}2\pi\alpha t}\mathrm{d}t\\&=2\pi A^2\mathrm{e}^{-\mathrm{j}2\pi f_0\tau}\delta(2\pi\alpha+2\pi K\tau)+2\pi R'_{\mathrm{n}}(\tau)\delta(2\pi\alpha)\end{aligned} \tag{4}$$

where α is the cyclic frequency. We can get its modulus

$$|R_{\mathrm{s}}^{\alpha}(\tau)|=\begin{cases}2\pi|A^2\mathrm{e}^{-\mathrm{j}2\pi f_0\tau}+R'_{\mathrm{n}}(\tau)|, & \alpha=0,\tau=0\\ 0, & \alpha\neq0,\tau=0\\ 2\pi|R'_{\mathrm{n}}(\tau)|, & \alpha=0,\tau\neq0\\ 2\pi A^2\delta(2\pi\alpha+2\pi K\tau), & \alpha\neq0,\tau\neq0\end{cases} \tag{5}$$

It is shown from Eq. (5) that the local α is determined by dividing the peak value by the lag τ. For the non-zero lag, i.e., $\tau\neq0$, these maxima corresponding to the signal energy and Gaussian white noise energy occur at the cyclic frequency $\alpha=-K\tau$ and $\alpha=0$, respectively. The conventional estimation method for the chirp rate involves searching the maximum of the cyclic autocorrelation function for a family of discrete values of τ and generates a sequence of α values, which suffers a large amount of calculation.

From Ref.[12], we know that the selection of a lag τ could affect the performance of the rate estimation of combined signal. When $\tau\to N/(2f_{\mathrm{s}})$, the estimation scheme delivers a better performance, where N is the total sampling points, and f_{s} the sampling frequency. The optimal performance of estimation appears at $\tau=N/(2f_{\mathrm{s}})$. Unfortunately, the phase ambiguity would emerge unless it meets $|b_2|\leqslant|\pi/(2\tau')|$,[3] where $b_2=\pi K/f_{\mathrm{s}}^2$, $\tau'=\tau f_{\mathrm{s}}$. Then the inequality becomes

$$|K|\leqslant\frac{f_{\mathrm{s}}}{2\tau} \tag{6}$$

Substituting $\tau=N/(2f_{\mathrm{s}})$ and $K=B/(N/f_{\mathrm{s}})$ into Eq. (6), where B is the bandwidth, then we can rewrite Eq. (6) as $B\leqslant f_{\mathrm{s}}$, which meets the band-pass Nyquist sampling theorem undoubtedly. It is evident to suggest that there is no phase ambiguity under general sampling when we make the optimal lag $\tau=N/(2f_{\mathrm{s}})$. Then, the chirp rate is obtained according to one-dimensional peak search with respect to the cyclic frequency, i.e., α. For an optimal, select non-zero lag τ and non-zero α of Eq. (5), and the rate of the CPPM-LFM can be obtained by

$$\widehat{K}=-\alpha/\tau \tag{7}$$

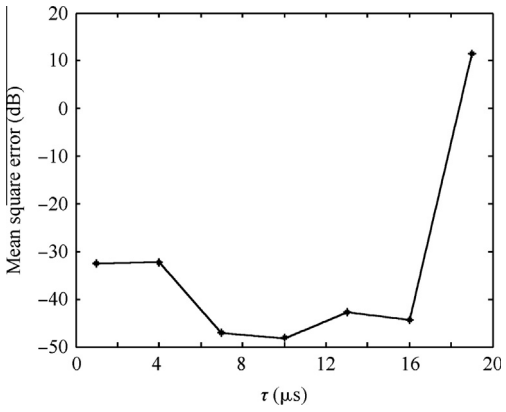

Fig. 1 Comparison of chirp rate estimates with different values of τ.

The following example shows the mean square error (MSE) of chirp rate estimation under the conditions of different values of τ in Fig. 1. 500 Monte Carlo trials were performed on the observed intra-pulse signal. The initial frequency $f_0 = 20$ MHz, $f_s = 100$ MHz, $N = 2000$, SNR $= -5$ dB, $K = 0.25 \times 10^{12}$ Hz/s. The proposed method deteriorates as the lag grows apart from $N/(2f_s)$, i.e., 10 μs as shown in Fig. 1. Simulation result assesses the effect of the lag election as expected. Take $\tau = N/(2f_s)$ as an example to illustrate our Eq. (5), and the peak of the signal energy in the correlation domain locates at $\alpha = -2.49$ MHz, as presented in Fig. 2. The satisfied estimate of the chirp rate, $\widehat{K} = 0.249 \times 10^{12}$ Hz/s, is derived from Eq. (7).

Having the estimated $\widehat{K}$, the received radar signal can be demodulated

$$y_s(t) = x_s(t)e^{-j\pi\widehat{K}t^2} = e^{j2\pi f_0 t + j\pi(K-\widehat{K})t^2} + n'(t) \tag{8}$$

where $n'(t) = n(t)e^{-j\pi\widehat{K}t^2}$. It can be seen that the demodulation signal is nearly a tone, when the estimation of $\widehat{K}$ is precise. $y_s(t)$ can be expressed in a discrete-time signal form as $y_s(n_1) = e^{j2\pi f_0 n_1/f_s + j\pi(K-\widehat{K})n_1^2/f_s^2} + n'(n_1), \quad n_1 = 1, 2, \ldots, N.$ We make Fourier coefficients interpolation of $y_s(n_1)$ to get the initial frequency estimation. The process is as follows:

Firstly, getting the Fourier transform of demodulation signal, $Y(n_1)$, we search for the index $l = \arg\max_{n_1}\{Y(n_1)\}$. The true frequency can be expressed as $f = \dfrac{(l+\delta)}{N} f_s$, where δ is a residual in the interval $[-0.5, +0.5]$. The estimate of δ is given by $\hat{\delta} = h(\delta) = \dfrac{1}{2}\mathrm{Re}\left\{\dfrac{S_{+0.5} + S_{-0.5}}{S_{+0.5} - S_{-0.5}}\right\}$, and the specific procedure can be seen in Ref.[13].

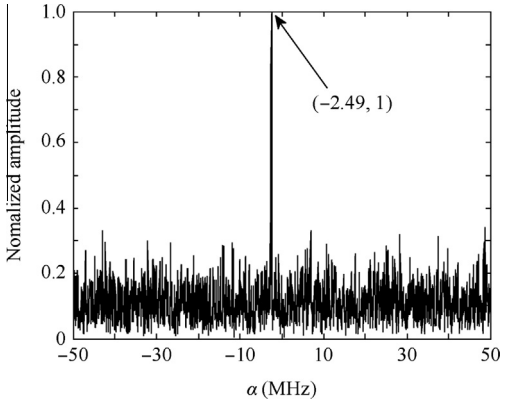

Fig. 2 Signal energy in correlation when $\tau = N/(2f_s)$.

The parameters of CPPM-LFM intra-pulse signal are extracted by the above mentioned methods. Unfortunately, the cyclic autocorrelation approach is not stable in low SNR. Simulations demonstrate this phenomenon. In this paper, a modified CHT estimation algorithm implementing HT is proposed.

3.2. HT method

HT, in essence, maps different points of a straight line in Cartesian coordinate to a family of sinusoids in 2D parameter space[14]. The straight line equation in the inclined cutting form is expressed as

$$y = ax + b \tag{9}$$

where a is the slope of the line, b the y-intercept. Cartesian coordinate transform is

$$\rho = x\cos\theta + y\sin\theta, \ \ \rho \geqslant 0, \ \ 0 \leqslant \theta \leqslant 2\pi \tag{10}$$

where ρ is the perpendicular distance from the origin to the line and θ the angle between line and x axis. The features of the line are mapped into parameter space using Eq. (10). Each point (x, y) will generate a different surface in the parameter space, but all surfaces generated by the points of a line will intersect at the common point which can describe the features of the line. Therefore, through an intelligence collection system, we can collect the parameter estimates of multiple pulses. A majority of the estimates are approximately equal and can be considered as a straight line paralleling to the x-axis, while the estimates with great error stand apart from the line. Thus, the outliers are removed through HT and the modified estimate which is nearly equal to the majority is achieved. The specific procedures of estimate modification via HT are as follows:

Step 1. The parameter space is composed of $p \times q$ basic units, where p is the equal interval number of θ, and q is the equal interval number of ρ Set an accumulator $Q_{p\times q}$.

Step 2. Set (i, y_i) as a point in the image space, where i is the ith pulse, and y_i the corresponding parameter estimate. Make Cartesian coordinate transform through Eq. (9) and calculate ρ with cells of this quantized space and then increase a counter connected with this cell, $Q(i_1, i_2) = Q(i_1, i_2) + 1$.

Step 3. When all the estimates are calculated after Step 2, through finding the maximum number of counts of accumulator cells, we can get the point $(\theta_{\mathrm{opt}}, \rho_{\mathrm{opt}})$ which is intersected at. Substituting Eq. (10) into Eq. (9) leads to

$$\begin{cases} a = -\cos\theta_{\mathrm{opt}}/\sin\theta_{\mathrm{opt}} \\ b = \rho_{\mathrm{opt}}/\sin\theta_{\mathrm{opt}} \end{cases} \tag{11}$$

Fitting the straight line where the vast majority of estimates are, we could get the value of b, i.e., the modified estimate. Here, HT is used to remove the outliers of the estimates of K and f_0.

4. Prediction of PRI based on Volterra adaptive filter

For the CPPM signal, the information is contained in the intervals between the pulses, which are determined by chaotic dynamics of a pulse generator[1]. The pulse occurrence time of CPPM-LFM signal can be obtained via many standard methods, such as energy detection algorithm.[15] In view of the fact that the PRI sequence of CPPM-LFM signal is highly nonlinear, the PRI prediction becomes a nonlinear prediction problem. These approaches which are able to capture the nonlinear reactor behavior mainly fall into two categories: neural networks and Volterra series expansion. For the neural networks, the huge computational loads are prohibitive for practical applications on electronic counter measures (ECM). Hence, the low-order Volterra filter, which offers reduction in the computational burden and approximate nonlinear systems efficiently, is applied to the PRI prediction of CPPM-LFM signal.

Firstly, normalize the detected PRI sequence, denoted by $\mathrm{PRI}(n)$, $n = 1, 2, \cdots, N-1$. The quantization does not affect the desirable properties of the sequence. Secondly, we reconstruct the state space that is the fundamental to describe a dynamic system,[16] and make $N_0 = n - (m-1)\tau_0$, where m is the embedding dimension and τ_0 the time lag. The vector based on the state space reconstruction is expressed as

$$\begin{aligned}\boldsymbol{W}(l_1) &= [\mathrm{PRI}(l_1)\ \mathrm{PRI}(l_1+\tau_0)\cdots\mathrm{PRI}(l_1+(m-1)\tau_0)]\\ l_1 &= 1, 2, \cdots, L-(m-1)\tau_0-1\end{aligned} \tag{12}$$

Where $\boldsymbol{W}$ is the state vector. Find the center vector of the reconstructed phase space, specifically

$$\begin{aligned}\boldsymbol{W}(N_0) &= [\mathrm{PRI}(N_0)\,\mathrm{PRI}(N_0+\tau_0)\cdots\mathrm{PRI}(N_0+(m-1)\tau_0)]\\ &= [\mathrm{PRI}(n-(m-1)\tau_0)\,\mathrm{PRI}(n-(m-2)\tau_0)\cdots\mathrm{PRI}(n)]\end{aligned} \tag{13}$$

Suppose the observation sequence of radar receiver is $\boldsymbol{W}_1(n) = [\mathrm{PRI}(n)\ \mathrm{PRI}(n-1)\ \cdots\ \mathrm{PRI}(n-N+1)]$. The Volterra series expansion of the chaotic system can be written in the form

$$\begin{aligned}\mathrm{PRI}(n+1) = F(\boldsymbol{W}_1(n)) = h_0 + \sum_{p=1}^{P}\sum_{t_1=0}^{S-1}\sum_{t_2=0}^{S-1}\cdots\\ \sum_{t_p=0}^{S-1}h_p(t_1, t_2, \cdots, t_p)\prod_{i=1}^{p}\mathrm{PRI}(n-t_i)\end{aligned} \tag{14}$$

where $F(\cdot)$ is the prediction model evolved from the original system, P the model order and S the memory length with the filter. The Volterra model kernel refers to $h_p(t_1, t_2, \ldots, t_p)$. The expansion is represented as a function of inputs $\mathrm{PRI}(n)$, which have an effect on the current output $\mathrm{PRI}(n+1)$.

One common difficulty involving the determination of the Volterra kernels encounters, when we want to apply the Volterra functional representation to nonlinear problem. The major shortcoming of this structure is that the number of parameters increases largely as the model order increases. Considering that the pulse position modulation (PPM) of radar signal is generally a chaotic set in a low dimension, the SOV and TOV models can characterize the inherent physical relationships of the chaotic PRI sequence. In addition, Ref.[17] points out that a high kurtosis and variance sequence could excite the third-order off-diagonal term selectively. Also, it can compensate the effects of the second-order off-diagonal terms relatively insignificant. However, the TOV model suffers more computational complexity. With a comprehensive consideration, it is worthwhile to analyze and compare both of them through the prediction achievement. Takens' embedding theorem[16] says that the dynamic system behavior can be described completely when $m \geqslant 2D_2 + 1$, where D_2 is the dynamic dimension. Therefore, we can set $S = m = 2D_2 + 1$.

The expansion of the SOV series in Ref.[7] is expressed as

$$\begin{aligned}\mathrm{PRI}(n+1) &= h_0 + \sum_{i_3=0}^{S-1}h_1(i_3)\mathrm{PRI}(n-i_3) + \sum_{i_3=0}^{S-1}\sum_{i_4=0}^{S-1}h_2(i_3, i_4)\mathrm{PRI}(n-i_3)\mathrm{PRI}(n-i_4)\\ &= \boldsymbol{H}_2^{\mathrm{T}}(n)\boldsymbol{U}_2(n)\end{aligned} \tag{15}$$

where $\boldsymbol{U}_2(n) = [1\ \mathrm{PRI}(n)\ \ldots\ \mathrm{PRI}(n-\mathrm{S}+1)\ \mathrm{PRI}^2(n)\ \mathrm{PRI}(n)\cdot\mathrm{PRI}(n-1)\ldots\mathrm{PRI}^2(n-S+1)]^{\mathrm{T}}$ is the input vector of Volterra adaptive filter, and the corresponding coefficient vector refers to $\boldsymbol{H}_2(n) = [h_0\ h_1(0)\ h_1(1)\ \cdots\ h_1(S-1)\ h_2(0,0)\ h_2(0,1)\ \cdots\ h_2(S-1, S-1)]^{\mathrm{T}}$.

In Ref.[18], when the nonlinear systems are predicted by the third-order architecture, a portion of the filter vector parameters converges to zero approximately, and these could be neglected. Consequently, the nonlinear models which predict the chaotic sequence can be taken as a sparse Volterra series expansion. The sparse TOV series are obtained as follows:

$$\begin{aligned}\mathrm{PRI}(n+1) &= h_0 + \sum_{i_3=0}^{S-1}h_1(i_3)\mathrm{PRI}(n-i_3)\\ &\quad + \sum_{i_3=0}^{S-1}\sum_{i_4=0}^{S-1}h_2(i_3, i_4)\mathrm{PRI}(n-i_3)\mathrm{PRI}(n-i_4)\\ &\quad + \sum_{i_3=0}^{S-1}h_3(0, i_3)\mathrm{PRI}^3(n-i_3)\\ &\quad + \sum_{i_3=1}^{S-1}h_3(1, i_3)\mathrm{PRI}^2(n)\mathrm{PRI}(n-i_3)\\ &\quad + \sum_{i_3=1}^{S-1}h_3(2, i_3)\mathrm{PRI}(n)\mathrm{PRI}^2(n-i_3)\\ &= \boldsymbol{H}_3^{\mathrm{T}}(n)\boldsymbol{U}_3(n)\end{aligned} \tag{16}$$

where $\boldsymbol{U}_3(n)$ and $\boldsymbol{H}_3(n)$ represent the input vector and the corresponding coefficient vector of the TOV filter, respectively.

Finally, the kernels of the SOV and TOV model can be identified using LMS algorithm,[19] which modifies the estimated coefficients of the filter adaptively using the information contained in new data samples to update the old estimates in the training process. Obtain the coefficients of linear adaptive finite impulse response (FIR) filter eventually. The iterative formula is given by

$$\begin{cases}\mathrm{PRI}(n) = \boldsymbol{H}^{\mathrm{T}}(n-1)\boldsymbol{U}(n-1)\\ \boldsymbol{H}(n) = \boldsymbol{H}(n-1) + \mu\boldsymbol{e}(n-1)\boldsymbol{U}(n-1)\\ \boldsymbol{e}(n) = \mathrm{PRI}(n) - \hat{\mathrm{PRI}}(n)\end{cases} \tag{17}$$

where μ is the step size, and $\hat{\mathrm{PRI}}(n)$ the predictive value.

Based on the prediction information, the next pulse position of CPPM-LFM signal can be obtained as

$$c_l = \sum_{l'=1}^{l-1}\mathrm{PRI}(l') \tag{18}$$

which is beneficial to further signal sorting of radar reconnaissance system.

5. Simulation results and discussion

The following simulation experiments are used to assess the validity of the proposed methods. In the experiment, $n(t)$ is a zero-mean white Gaussian noise, the initial frequency of CPPM-LFM signal $f_0 = 20$ MHz, $K = 0.25 \times 10^{12}$ Hz/s, $N = 2000$, $f_s = 100$ MHz, $p = 180$ and $q = 1000$ in HT, 100 Monte Carlo runs. The Logistic, Lorenz and Henon map are taken as the chaotic sequences of PPM, the pulse number $L = 101$.

The experiments are realized under the SNR values ranging from -6 dB to 11 dB. The MSEs of K and f_0 estimation are shown in Figs. 3 and 4, respectively. In Figs. 3 and 4, "C correlation" represents the cyclic autocorrelation approach[3], "Q dechirp" is the quick dechirp method[2] by means of delay conjugate multiplication, and "CHT" the proposed cyclic autocorrelation HT algorithm.

Fig. 3 presents that when SNR is less than -4 dB, for the slope K estimation, the presented CHT algorithm delivers about 60 dB MSE improvement upon quick dechirp method. Whereas, about 10 dB worse when SNR $\geqslant -4$ dB. Compared with the cyclic autocorrelation method, CHT has the equal estimation ability. In fact, the parameter estimation of LFM signal using HT achieves good performance in low SNR (more than -12 dB). Considering the application of the pulse position prediction, much lower SNR region is not discussed in the paper. Fig. 4 shows that the proposed CHT method for f_0 estimation has 8 dB higher precision than cyclic autocorrelation method in the case of SNR $\geqslant -6$ dB. In contrast with the quick dechirp method, CHT delivers a superior MSE improvement (about 50 dB) when SNR $= -6$ dB. Note that there is still 5 dB promotion in more than -6 dB SNR region due to the Fourier coefficients interpolation. The simulation results illustrate that the proposed approach has a certain anti-noise performance by means of the realizations to efficiently remove the outliers of the estimates by HT.

Subsequently, the PRI sequence of CPPM-LFM radar signal is predicted by the SOV and TOV adaptive filters. The former normalized 100 PRI data are used as the training samples. In order to illustrate the stability of the proposed methods, we consider the performance comparison of two predictive models, as shown in Tables 1 and 2. One phenomenon in the simulation results is that the prediction schemes deteriorate when SNR is less than -3 dB, mainly because chaotic signal is sensitive with the initial values corrupted with noise. When SNR $\geqslant -1$ dB, the prediction errors of three chaotic signals change only a little In addition, it is interesting to note that the MSE of Logistic and Henon map via the SOV prediction architecture is superior to that obtained by the TOV model, since the Logistic and Henon map have lower dimensional linear degrees and complexity cost compared with the Lorenz map. Nevertheless, such condition inverses for the Lorenz map. In reality, the Volterra series expansion based on second-order statistics is able to describe Lorenz architecture although not as accurately as the TOV method, whereas, considering the low cost, they are definitely a bargain. Note that there is no prior knowledge for a radar reconnaissance system, thus, the SOV adaptive prediction scheme predetermined to

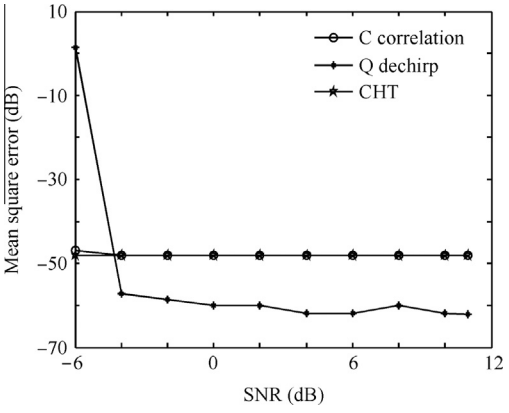

Fig. 3 MSE for slope estimation.

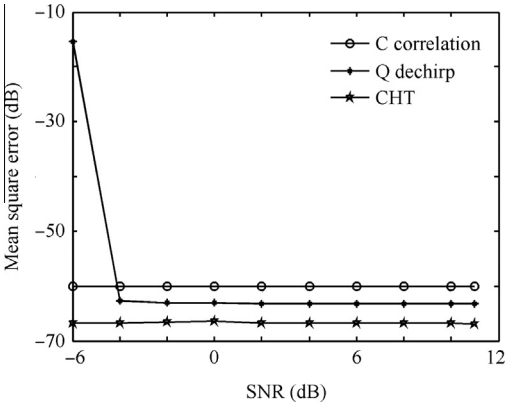

Fig. 4 MSE for initial frequency estimation.

Table 1 MSE summary of SOV adaptive prediction (10^{-3}).

SNR(dB)	Chaotic sequence of the PPM (10^{-3})		
	Logistic	Henon	Lorenz
−6	202.3	150.4	143.4
−3	0.4122	0.2482	0.1834
−1	0.2861	0.1766	0.1469
1	0.2369	0.1381	0.1165
3	0.1978	0.1149	0.0967
5	0.1721	0.0923	0.0679
7	0.1471	0.0809	0.0579
9	0.1405	0.0764	0.0529
11	0.1352	0.0721	0.0506

Table 2 MSE summary of TOV adaptive prediction (10^{-3}).

SNR(dB)	Chaotic sequence of the PPM (10^{-3})		
	Logistic	Henon	Lorenz
−6	204.4	150.2	150.2
−3	0.3917	0.5943	0.08424
−1	0.2813	0.1970	0.05812
1	0.2311	0.1456	0.05147
3	0.1920	0.1221	0.04040
5	0.1596	0.1059	0.03048
7	0.1374	0.0971	0.02534
9	0.1230	0.0806	0.02029
11	0.1195	0.0792	0.02011

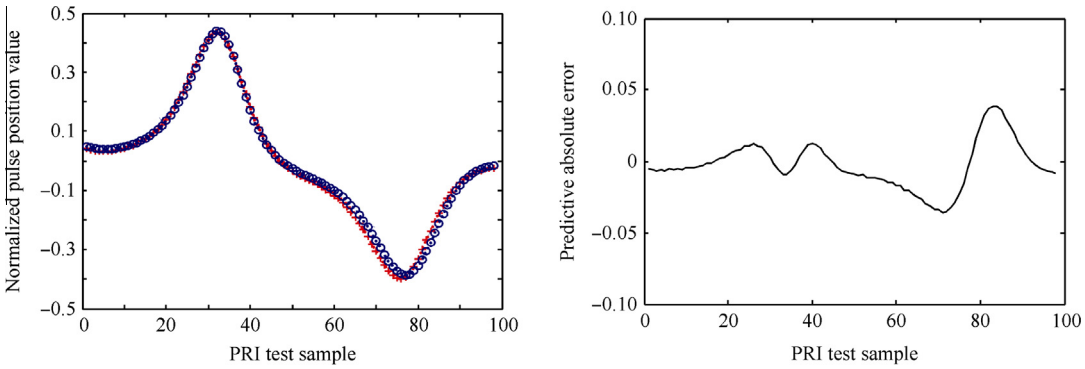

(a) PRI prediction of combined signal (b) Predictive absolute error

Fig. 5 Prediction of PRI via TOV adaptive filter.

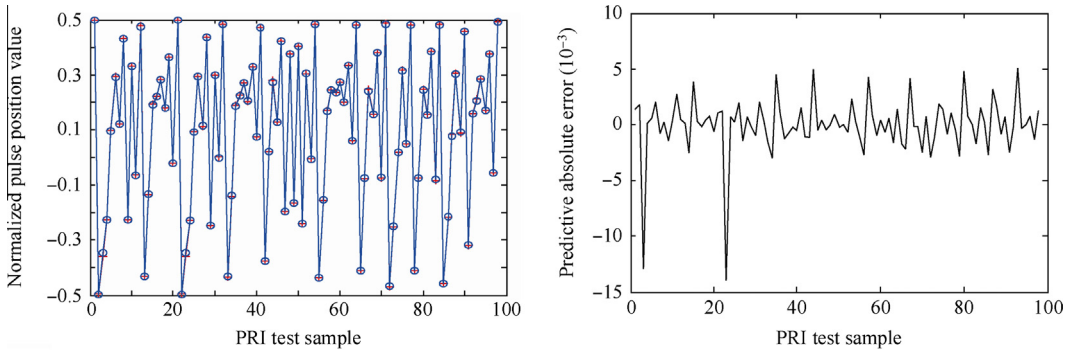

(a) PRI prediction of combined signal (b) Predictive absolute error

Fig. 6 Prediction of PRI via SOV adaptive filter.

forecast the chaotic PPM signal's position is an optimal process.

For ease of observation and comment, Lorenz and Henon map PPM signal are taken as examples to illustrate the proposed methods. Fig. 5 provides an illustrate depiction of the PRI predictive effect of the Lorenz map PPM signal via the TOV adaptive filter ($\tau_0 = 3$, $S = 3$). Fig. 6 portrays the predictive effect of PRI employing the SOV adaptive filter while the pulse position is modulated by the Henon map ($\tau_0 = 1$, $S = 2$). Where " + " denotes the real values, and "O" the predictive values. The simulation environment SNR = 0 dB. It is observed that the low-order Volterra adaptive filter does an efficient job of the PRI prediction of CPPM-LFM signal corrupted by white Gaussian noise. Finally, the pulse position c_l could be estimated according to Eq. (18).

6. Conclusions

(1) The proposed CHT algorithm is used to estimate the intra-pulse parameters of the combined CPPM-LFM signal in the low SNR.
(2) Model-based predictive algorithm by means of Volterra adaptive filter for three chaotic PRI sequences can predict well when SNR $\geqslant -3$ dB.
(3) The key properties obtained from the employment of the Volterra model in the chaotic system is the fact that the SOV and TOV adaptive filters make comprehensive utilization of the linear and nonlinear factors and the high-order moment information.

Acknowledgment

This work is supported by the National Natural Science Foundation of China under Grant 61172116.

References

1. Rulkov NF, Sushchik MM, Tsimring LS. Digital communication using chaotic-pulse-position modulation. *IEEE Trans Circ Syst I Fund Theor Appl* 2001;**48**(12):1436–44.
2. Peleg S, Porat B. Linear FM signal parameter estimation from discrete-time observations. *IEEE Trans Aerosp Electron Syst* 1991;**27**(4):607–16.
3. Shamsunder S, Giannakis GB, Friedlander B. Estimating random amplitude polynomial phase signals: a cyclostationary approach. *IEEE Trans Signal Process* 1995;**43**(2):492–505.
4. Kaihui D, Qun D, Run Zhe L. Parameters estimation of LFM signal based on fractional order cross spectrum. In: *Proceedings of the electronic and mechanical engineering and information technology (EMEIT) international conference*, 2011. p. 654–6.
5. Alonge F, Branciforte M. A novel method of distance measurement based on pulse position modulation and synchronization of

chaotic signals using ultrasonic radar systems. *IEEE Trans Instrum Meas* 2009;**58**(2):318–29.
6. Fortuna L, Frasca M, Rizzo A. Chaos preservation through continuous chaotic pulse position modulation. In: *The 2001 IEEE international symposium on circuits and systems*, 2001. p. 803–6.
7. Haiquan Z, Jiashu Z. A novel adaptive nonlinear filter-based pipelined feedforward second-order Volterra architecture. *IEEE Trans Signal Process* 2009;**57**(1):237–46.
8. Kuech F, Kellermann W. Partitioned block frequency-domain adaptive second-order Volterra filter. *IEEE Trans Signal Process* 2005;**53**(2):564–75.
9. Krall C, Witrisal K, Leus G. Minimum mean-square error equalization for second-order Volterra systems. *IEEE Trans Signal Process* 2008;**56**(10):4729–37.
10. Nichols JM. Frequency distortion of second- and third-order phase-locked loop systems using a Volterra-series approximation. *IEEE Trans Circuits Syst I Regular Papers* 2009;**56**(2):453–9.
11. Gu J, Chen X, Zhou J. An algorithm of predictions for chaotic time series based on Volterra filter. In: *Second international symposium on electronic commerce and security*, 2009. p. 205-08.
12. Morelande MR, Zoubir AM. On the performance of cyclic moments-based parameter estimators of amplitude modulated polynomial phase signals. *IEEE Trans Signal Process* 2002;**50**(3):590–606.
13. Aboutanios E, Mulgrew B. Iterative frequency estimation by interpolation on Fourier coefficients. *IEEE Trans Signal Process* 2005;**53**(4):1237–42.
14. Daming S, Liying Z, Jigang L. Advanced Hough transform using a multilayer fractional Fourier method. *IEEE Trans Image Process* 2010;**19**(6):1558–66.
15. Boksiner J, Dehnie S. Comparison of energy detection using averaging and maximum values detection for dynamic spectrum access. In: *34th IEEE Sarnoff Symposium*, May 3–4, Princeton, NJ. 2011. p. 1–6.
16. Takens F. Detecting strange attractors in turbulence. *Dyn Syst Turbul* 1980;366–81.
17. Soni AS, Parker RS. Control relevant identification for third-order Volterra systems: a polymerization case study. In: *Proceedings of American control conference*, 2004. p. 4249–54.
18. Hong-Zhou T, Aboulnasr T. TOM-based blind identification of nonlinear Volterra systems. *IEEE Trans Instrum Meas* 2006;**55**(1):300–10.
19. Godavarti M, Hero AO. Partial update LMS algorithms. *IEEE Trans Signal Process* 2005;**53**(7):2382–99.

Zhang Wei received the B.S. degree in Northeast Dianli University. She is a postgraduate in School of Electronic Engineering, University of Electronic Science and Technology of China (UESTC). Her research interests include radar electronic reconnaissance, signal detection and parameter estimation, etc.

Xiong Ying is a senior engineer in University of Electronic Science and Technology of China. Her research interests are ECM and ECCM of radar.

Wang Pei received the B.S. degree in information warfare technology in University of Electronic Science and Technology of China (UESTC) in 2010, and now is a Ph.D. candidate in School of Electronic Engineering, UESTC. His research interests are detections and classifications of radar signals, parameter estimations of complicated modulated LPI signals.

Wang Jun is a senior engineer in University of Electronic Science and Technology of China. His research interest is digital signal processing.

Tang Bin received his Ph.D. degree from the University of Electronic Science and Technology of China (UESTC) and now is a professor and Ph.D. supervisor in UESTC. His research interests are ECM and ECCM of radar and communication.